J Mater Sci (2010) 45:3318–3324
DOI 10.1007/s10853-010-4349-z

Sonochemical synthesis of silver nanoparticles in Y-zeolite substrate

Jafar Talebi · Rouein Halladj · Sima Askari

Received: 31 October 2009 / Accepted: 23 February 2010 / Published online: 9 March 2010

Abstract Silver ions can be reduced by 24 kHz ultrasonic waves in ion-exchanged Ag^{+}–Y zeolite. In this research, silver ions were introduced into the nano-porous (1.2 nm) zeolite lattice by ion-exchange route. After the reduction process, silver nanoparticles were placed in the cavities, with a size of about 1 nm and also on the external surfaces of the zeolite, with sizes about less than 10 nm. Fast and simple lab-scale reduction of silver ions in the zeolite is important for researchers who work on catalytic properties of metallic silver–zeolite. Several reduction methods have been reported but reduction by ultrasonic waves is a new, simple, and size-controllable method with a high practical value which does not need any complicated facilities. In a sonochemical process, a huge density of energy is provided by the collapse of bubbles which formed by ultrasonic waves. The released energy causes the formation of reducing radicals that consequently reduce the silver ions. It is concluded that the higher silver content may result in the formation of larger silver crystals on the external surface of zeolite crystals. Also, the addition of 1-propanol and 2-propanol to the aqueous reaction medium does not cause better reduction. In addition, increasing the irradiation time and ultrasonic power does not affect the silver crystal growth significantly but the extent of silver ion reduction increases when the power of ultrasonic waves increases. All samples were irradiated under the same ultrasonic conditions. The samples were analyzed by XRD, EDS, SEM, and TEM.

J. Talebi · R. Halladj (✉) · S. Askari
Chemical Engineering Department, Amirkabir University of Technology, P.O. Box 15875-4413, Hafez Ave, Tehran, Iran
e-mail: halladj@aut.ac.ir

Introduction

Nowadays the importance of nanoparticles and their uses in different industries have attracted many researches. The materials in nano-scale show different characteristics in comparison with their bulk state. Among various nanoparticles, transition metal ones are so interesting because of their unique physico-chemical properties [1]. Silver, as one of the transition elements, has lots of uses in the fields of electronics, magnetism, catalysis, medicine, dentistry, food, and construction industries [2, 3].

Furthermore, introducing a single nanoparticle into other materials would result in a system with new uses. These systems are called nanocomposites [4]. Depending on the phases of constituents, we have several kinds of nano-composites such as: metal–polymer (e.g. Ag in polystyrene, Teflon, etc.) [4–7], metal–metal (e.g. Pd/Fe, Pt/Co, Ru/Co, Ag/Bi, etc.) [8], metal–metal oxides or ceramics (e.g. Pt, Pd, Cu, Co, Fe, Ni, and Ag on SiO_2, Al_2O_3, and TiO_2) [9], and metal–zeolite (e.g. Ag–ZSM5, Ag–Y, etc.) [10]. Nanocomposite properties depend on the properties of single constituents, the particle size, shape, and the interaction of surfaces. Nanocomposites enable us to have a variety of different properties in one place and also, the hardness and erosion resistance of metals such as silver can be improved by using them. Zeolite as a porous solid is a good candidate for accepting silver as a guest.

The importance of making silver–zeolite nanocomposites and reduction of silver in the zeolite is due to nanopores in the zeolite framework which help us to control the particle size and to have a uniform distribution of silver metals on the internal and external surfaces. These factors are very important for nanocatalysts [1]. The capabilities of silver–zeolite composites are much enough to make studying them reasonable. Some of their uses are: formaldehyde production

by methanol oxidation [2], making anti-bacterial and anti-microbial coatings [3], decomposition of ozone gas at ambient condition [9], photo-catalytic decomposition of NO_x [10], making humidity sensors [11], photo- or thermo-chemical decomposition of water to hydrogen and oxygen [11, 12], catalytic conversion of methane in the presence of ethene [13], oxygen production by N_2 adsorption from air [14], cumene cracking [15], adsorption and oxidation of CO [16], adsorption of unreacted hydrocarbons from automobile engines [17], drinking water production from saline water [18], adsorptive removal of dimethyl sulfide and *t*-butyl mercaptan from natural gas pipelines at ambient condition [19], desulfurization of fuels (gasoline, diesel and jet fuel) [20], improving gasoline octane number in alkylation process [21], adsorption of chemical warfare agents [22], etc. In these examples, the state of silver in the zeolite framework is either ionic or metallic.

Zeolites are alomino-silicate compounds which are made of TO_4 (T = Si and Al) hexagonal linking together by oxygen atoms and have a lot of channels and pores. Cations and water molecules are other species that are present in the zeolite cavities. Cations balance the negative charge of zeolite lattice and are exchangeable with other cations. Also, water molecules can be removed from the lattice by simply heating the zeolite [23]. The zeolites themselves have lots of uses in petrochemical industry [9]. Type Y zeolite is one of important zeolites that has relatively high ion-exchange capacity, lattice stability and also, plenty of researches have been done on its structure and its interactions with different cations [23]. Y-zeolite has three kinds of pores: supercages with a pore opening of 7.4 Å and internal diameter of 12 Å, sodalite cage with a pore opening of 2.6 Å and internal diameter of 6.6 Å, and hexagonal prism with a pore opening of less than 2.6 Å [24].

Introducing silver ions into the zeolite framework is done by common methods of ion-exchange in silver nitrate solution [12, 23, 25, 26]. However, reducing silver ions and converting them to metallic form in the zeolite has different methods such as: reduction by heat [3], reduction by hydrogen [10], reduction by common reducing agents (e.g. hydrazine) [12], reduction by hydrocarbons [15], reduction by carbon monoxide [16], photo reduction [27], pulse sono-electrochemical reduction [28], and electrochemical reduction [29].

In addition to above methods, sonochemical reduction by ultrasonic irradiation (20 kHz–10 MHz [30]) is a new method for reducing metallic cations and making single nanoparticles or nanocoatings [31]. Contrary to previous methods, this method is very simple, fast, and does not need any complicated facilities. Also, this method can be used for industrial scale and recently there are some activities in this field [32–34]. In this method, the size of particles can be easily controlled by changing the initial concentration of precursors. Chemical effects of ultrasonic waves are due to cavitation phenomena in the solution. Generally, cavitation is the process of formation, growth, and collapse of bubbles in the liquid. Due to collapse of bubbles, a temperature and pressure of about 5,000–25,000 K and 181.8 MPa [1] are produced. Such a high temperature breaks the chemical bonds and consequently, causes the reactions to proceed. Collapsing of bubbles occurred in less than a nanosecond and so, a high rate of temperature decrease (10^{11} K/s) takes place, which prevents the organization and agglomeration of particles formed by ion reduction [30]. To explain the reduction mechanism of sonochemical reactions, three steps are suggested [35]: (i) reduction of ions by hydrogen atoms produced by ultrasonic irradiation of solution, (ii) reduction by secondary radicals produced due to removing of hydrogen from organic additives by OH radicals and H atoms, (iii) reduction by pyrolysis radicals that are produced by thermal decomposition of organic additives at the interface of cavitation bubbles and the solution (H atom is one of the strongest reducing agents that easily reduces the silver ions [36]). Also, the mechanisms that can describe how the above methods reduce silver ions are discussed in the mentioned references. A lot of parameters affect the sonochemical reaction and its products. Some of these effecting parameters are: frequency and power of ultrasonic waves, time of exposure to irradiation, solution temperature, type of solution, reaction vessel diameter, and the kind of noble gas used in the reaction environment [26, 37–39].

In this study, the sonochemical reduction of silver ions in silver–zeolite composite is investigated. Silver nanoparticles were produced on the external surface of zeolite crystals, with a size of about 10 nm and also, in the zeolite cavities with a size of about 1.2 nm (this is the size of zeolite cavities that is used to estimate the size of silver particles). Some parameters such as silver content, type of reaction media (alcoholic or aqueous), time of ultrasonic irradiation, and ultrasonic power, were studied. Lots of uses of this composite and also, the benefits of sonochemical method due to simply producing silver–zeolite samples in the lab-scale in order to study them in practical fields, made us eager to do this project. According to our information, the only work done about sonochemical reduction of metallic ions in the zeolite lattice is the preparation of palladium–zeolite (Pd–Y) nanocomposite [25, 26] and no report is present on sonochemical production of metallic silver–zeolite composite in the literature.

Experimental

The zeolite we used was Na^+–Y ($Na_{59.08}Al_{59.08}Si_{132.92}O_{384}\cdot xH_2O$) with a molar ratio of $SiO_2/Al_2O_3 = 4.5$. Ion-exchange was done by common method in silver nitrate

solution. For preparing the ionic silver–zeolite sample containing 33 wt% silver (Ag^+–Y-33), 2 g of Na^+–Y-zeolite was washed by distilled water and then stirred for 6 h with 160 mL $AgNO_3$ (0.05 M) at 35 °C. To have a completely ion-exchanged silver–zeolite, the samples were again mixed with fresh $AgNO_3$ solution at the same conditions. Finally, the Ag^+–Y-33 zeolite particles were filtered and then dried at 50 °C in an oven. All the steps were carried out in the absence of direct light. Another sample with 19 wt% silver content was also prepared in this way but with less contact time between the sample and the solution.

Ultrasonic irradiation was produced at 20 °C by an ultrasound generator (UP200H, 24 kHz, 80% pulse ratio, 600 W/cm^2) with a titanium sonotrode. To study the effect of silver content, ion-exchanged samples were mixed with distilled water in the reaction vessel that was placed in a water bath (300 mg per 100 mL). Air was discharged from the reaction vessel by passing the argon gas through the solution for 15 min before beginning the ultrasonic irradiation. Then the solution was irradiated for 2 h while the argon gas was flowing thorough the reaction solution (these conditions were the same for all of the samples). The sample that was used for other experiments was Ag^+–Y-33. In the case that 1-propanol and 2-propanol were presented as organic additives, at first, 1 mL of alcohol was added to the solution and then during the reaction, every 30 min, another 1 mL was added. The reaction time was 2 h for all the reaction solutions. To study the effect of ultrasonic irradiation time, the samples of the same conditions were irradiated for 2 h and 4 h. Finally, to study the effect of ultrasonic power, the power of ultrasonic generator was increased from 130 to 645 W by using two sonotrode with different diameters (3 mm∅ for 130 W and 14 mm∅ for 645 W). Again the reaction time was 2 h. Finally, the powders were centrifugally separated from the solution and dried at 50 °C in an oven.

The X-ray diffraction (XRD) patterns were recorded by Philips diffractometer with a copper anode and step sizes of 0.04° and 0.08°. The scanning electron microscopy (SEM) and energy dispersive X-ray spectroscopy (EDS) tests were done by Seron technology (AIS2100) scanning electron microscope. Also, the transmission electron microscopy (TEM) was done by a 120 kV Philips microscope (CM120).

Results and discussion

The silver content of ion-exchanged samples was determined by EDS. The sodium elements were not detected by EDS in Ag^+–Y-33 samples, indicating the complete ion-exchange of Na^+–Y (Fig. 1b). It is reported elsewhere that usually there are some ion-exchange sites (about 10–20% of total exchangeable sites) that are occupied with hydrogen and are not exchangeable with Ag^+.

After irradiation of ion-exchanged samples by ultrasound, it was seen clearly that their color changes from white to gray. The gray color of samples indicates the reduction of silver ions and formation of metallic silver crystals on the external surface of the zeolite crystals. Before the reduction process, Ag^+–Y samples have a little color change. Since silver ions have a high tendency to be reduced, it can be said that this color change is related to the auto-reduction of silver ions due to slight heating during the ion-exchange process. Other evidences of the ability of ultrasonic power to reduce the silver ions in the zeolite structure are the appearance of silver crystal peaks in the XRD patterns of the samples and production of silver nanoparticles on the external surface of zeolite crystals that is found in the TEM images.

In Fig. 2 a new peak at about $2\theta = 37°$ is appeared that is different from primary zeolite peaks (it is determined in the figure). This peak belonged to silver crystals (according

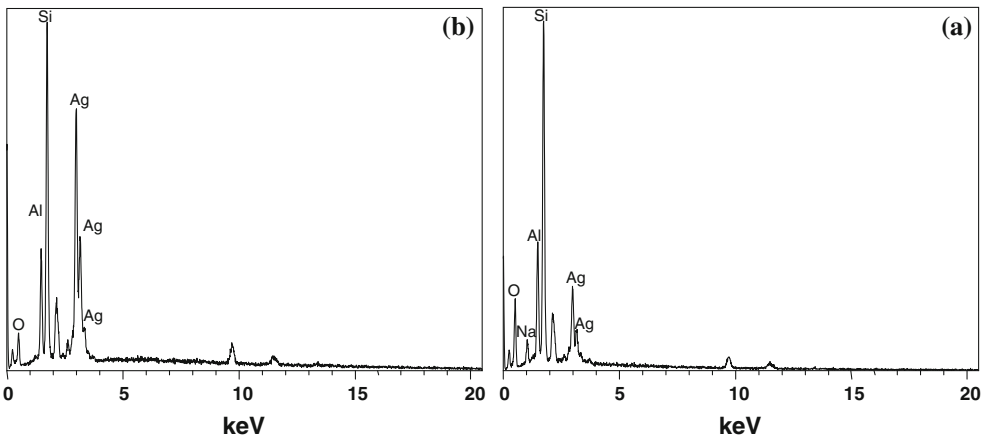

Fig. 1 The EDS spectra of ion-exchanged silver–zeolites with different silver content: **a** 19%, **b** 33%

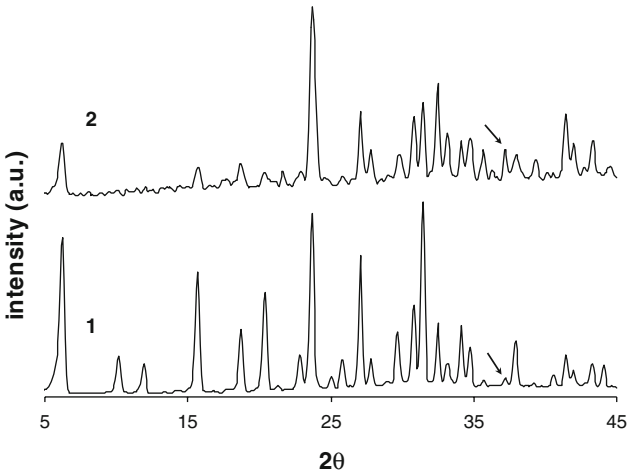

Fig. 2 The XRD pattern of (*1*) basic Na^+–Y-zeolite and (*2*) ion-exchanged sample that is reduced sonocheically (130 W, 2 h, aqueous reaction solution); the appearance of silver crystals peak is evidence

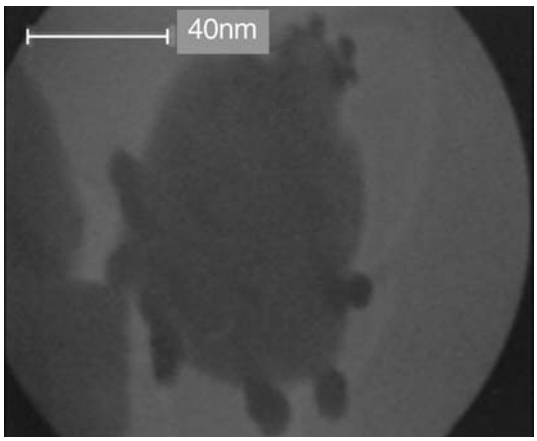

Fig. 3 The TEM image of a sonochemically reduced sample (645 W, 2 h, aqueous reaction solution); the silver nanoparticles are shown on the external surface of the zeolite crystals

to the silver standard diffraction pattern of NO. 41-1402) and clearly confirms the reduction of silver ions by ultrasonic irradiation and the formation of silver particles, as it is concluded from the color change of the samples after irradiation.

Since reduced silver atoms are weakly held in the zeolite cavities, because their ionic links are changed to weak Van Der Waals ones, they are easily moved out and begin to grow on the external surface. So some of the reduced silver atoms are in cavities with a size of about 1.2 nm and some of them are present on the external surface with a size of about 10 nm. Although the use of Scherrer formula shows that the average size of silver nanoparticles could be 97 nm but it is evident from the TEM images that particle sizes as small as 10 nm are also present on the external surface of zeolite crystals. It is concluded from the TEM image that is shown in Fig. 3. In this figure, the presence of silver nanoparticles is seen clearly on the external surface of zeolite crystals with sizes less than 10 nm. These spherical particles are distinguished from the zeolite crystals by their darker color. Although the size of particles are very small but they do not have a good distribution on the surface. The smaller silver particles that are placed in the zeolite cavities are not detected by TEM because zeolite crystals have a high electron density and so, the electrons produced by microscope cannot pass through the samples.

In addition to chemical effects of ultrasonic waves, their mechanical effects are also important. The collapse of cavitational bubbles results in the production of shock waves. These waves can erode the impacted surfaces. Thus, the structure of zeolitic samples will be affected. In Fig. 4, the SEM pictures of ion-exchanged sample containing 19% silver (Ag^+–Y-19) and its reduced form that is irradiated by ultrasound (Ag–Y-19) are shown. It is obvious that after the irradiation by ultrasound, some of the zeolite particles are broken into pieces. This is the mechanical effect of cavitation bubbles collapses. Beside these external zeolite structural changes, there is also, a little internal change in the zeolite lattice that is detected by XRD patterns.

The XRD test is one of the most important analyzing methods to study zeolites and reduced metallic particles in them. As shown previously in Fig. 2, some of the XRD peak intensities of ion-exchanged or reduced samples are decreased relative to the primary Na^+–Y-zeolite. It is because of changes in charge distribution and electrostatic fields that occurred when the sodium ions are replaced by silver ions. In addition, in comparison with primary zeolite, some peaks are not present in the XRD pattern of ion-exchanged or reduced samples. For example, there is a peak in the Na^+–Y pattern at $2\theta = 12°$ that it is not presented in other samples. In fact, the replacement of Na^+ with larger cations makes changes in the (311) surface (the ionic radius of Na^+ is 0.98 Å and that of Ag^+ is 1.13 Å). For achieving a suitable place in the high charge density zeolitic lattice, silver cations cause changes in the zeolite internal structure. But, almost all of the peaks are not changed, then it is concluded that the main internal structure of zeolite samples is fixed.

In Fig. 5, the XRD pattern of reduced samples with different silver content is compared. It is seen that the intensity of silver peaks in reduced form of Ag^+–Y-33 (i.e. Ag-Y-33) is more than that of Ag–Y-19; this is due to the result of changing the amount and crystal size of silver on the external surface of the zeolite framework. Consequently, low silver content in silver–zeolite samples results in the formation of smaller particles. Also, the peak intensity of zeolite crystals is a little reduced and some of them are wiped out. The reason is the increased destruction of zeolite structure by increasing the amount of silver ion

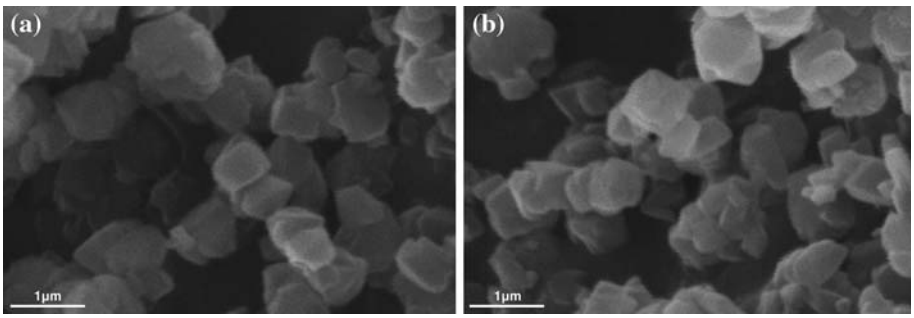

Fig. 4 The SEM image of samples containing 19% silver: **a** before and **b** after irradiation by ultrasound (130 W, 2 h, aqueous reaction solution)

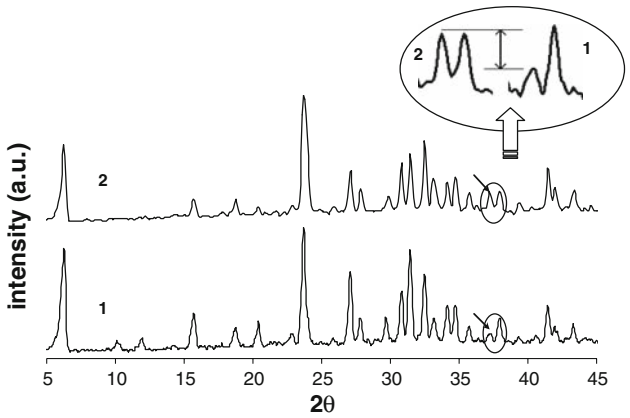

Fig. 5 XRD patterns of sonochemically reduced (130 W, 2 h and aqueous reaction solution) samples with different silver contents: (*1*) 19% and (*2*) 33%

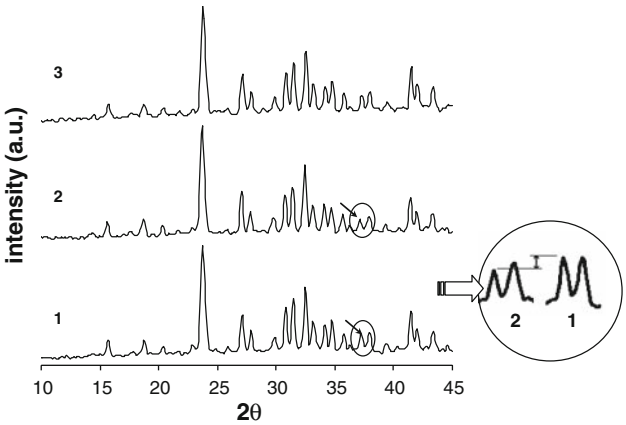

Fig. 6 XRD patterns of sonochemically reduced (130 W, 2 h) Ag–Y-33 in aqueous solutions containing: (*1*) no additives, (*2*) 1-propanol, and (*3*) 2-propanol

reduction and their increased migration to the surface. In addition, increasing the amount of ion-exchange in order to have higher silver content samples can cause more destruction in the zeolite structure.

The XRD peak intensity of reduced sample, Ag-Y-33, in water (without any additives) is more than the peak intensity of the samples that are reduced in the presence of organic additives (Fig. 6); it is an indication of better reduction of silver ions and better growth of silver atoms in aqueous solution. Different effects of the reaction solutions could be due to the larger size of radicals produced in the presence of 1-propanol and 2-propanol. The silver ions are confined in the zeolite cavities and so, the radicals have size limitations to access the silver ions. Thus, the smaller the size of the reducing radicals, the more amounts of silver ions reduced.

The reduction mechanism of silver ions, in the zeolite lattice by ultrasonic irradiation in the aqueous solution and also, in the presence of alcoholic additives (1-propanol and 2-propanol) is as follows:

$$H_2O \xrightarrow{\text{Sonication})))} {}^{\bullet}OH + {}^{\bullet}H \quad (1)$$

$$\begin{aligned} &CH_3(CH_2)_2OH + {}^{\bullet}OH({}^{\bullet}H) \rightarrow CH_3CH_2{}^{\bullet}CHOH + H_2O(H_2) \\ &(CH_3)_2CHOH + {}^{\bullet}OH({}^{\bullet}H) \rightarrow (CH_3)_2{}^{\bullet}CHOH + H_2O(H_2) \end{aligned} \quad (2)$$

$$\begin{aligned} &CH_3(CH_2)_2OH \xrightarrow{\text{pyrolysis}} \text{1-propanol pyrolysis radicals} \\ &(CH_3)_2CHOH \xrightarrow{\text{pyrolysis}} \text{2-propanol pyrolysis radicals} \end{aligned} \quad (3)$$

$$Ag^+ + \text{radicals} \rightarrow\rightarrow Ag^{\bullet} \quad (4)$$

$$n(Ag^{\bullet}) \rightarrow (Ag^{\bullet})_n \quad (5)$$

Equations 1–3 show the formation of radicals by sonochemical reactions. Other radicals like ${}^{\bullet}CH_3$ or $RO^{\bullet}$ may be formed. In the case that there are no additives in the reaction solution the only steps are (1), (4), and (5) and the main effective reducing radical is H atom. In Eq. 4, the Ag^+ cations are reduced by the produced radicals. Finally, the formation of silver crystals by agglomeration is shown in Eq. 5. As a matter of fact, there may be some unaffected silver ions that are not reduced during the reduction process. To determine the yield of silver atoms or the percent of silver reduction it is needed to do some extra tests like IR. This method is explained elsewhere [40].

The effect of irradiation time is another parameter that has been studied. The results show that there is not any considerable change in the size of silver crystals formed when the time is increased from 2 to 4 h because the peak intensity of Ag–Y-33 samples are not changed (Fig. 7).

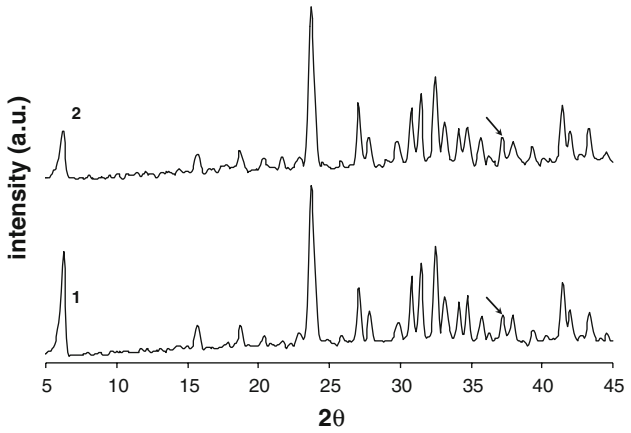

Fig. 7 XRD patterns of sonochemically reduced (130 W, aqueous reaction solution) Ag–Y-33 for (*1*) 2 h and (*2*) 4 h

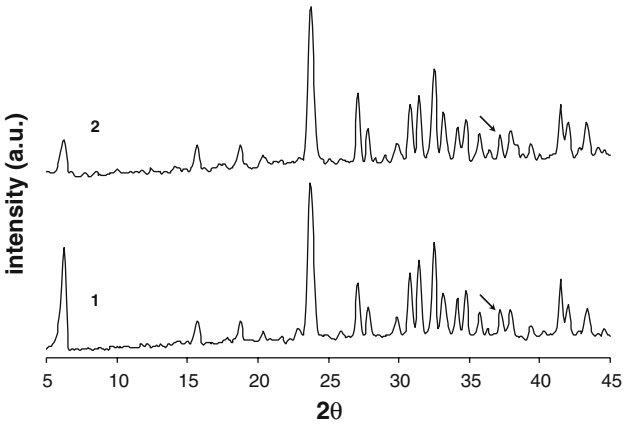

Fig. 8 The XRD patterns of the Ag–Y-33 sample reduced by different ultrasonic powers (2 h, aqueous reaction solution): (*1*)130 W and (*2*) 645 W

One of the reasons of this result may be the effect of cavitational bubble collapse. The shock waves that are produced as a result of bubble collapse may hit the reduced silver clusters and prevent their growth. So, depending on the power of ultrasonic waves, the growth of particles is limited. Also, the XRD pattern of the sample that is irradiated for 4 h has less intense peaks and so, the more contact time of the ultrasonic wave with the sample may cause much destruction in the zeolite structure.

The energy produced by the ultrasound generator was increased from 130 to 645 W by changing the sonotrode diameter from 3 to 14 mm. The increase in the ultrasonic power results in the higher turbulence of the reaction mixture. The Ag–Y-33 sample that is irradiated by the 14 mm sonotrode has a darker gray color. This is an indication of more silver ion reduction in the zeolite structure. This result is predictable because the increase in ultrasonic power may result in the increase of active radical production and so, more silver ions are reduced.

Comparison of XRD patterns of the two samples in Fig. 8 shows that there is no increase in the peak of silver crystals. This result shows that though the amount of silver reduction is increased, the size of silver crystals is not changed. So, increase in the power of shock waves limits the crystal growth.

Conclusion

Silver ions are reduced successfully by ultrasonic irradiation in the zeolitic structure. The formation of nanoparticles is detected by sample color change from white to gray, appearance of silver crystal peaks in the XRD patterns and TEM images. The silver nanoparticles are distributed both in the zeolite cavities (with a maximum size of 1.2 nm) and on the external surface of zeolite structure (with a size of less than 10 nm, according to the TEM image of reduced Ag–Y-33 with 645 W ultrasonic power). In addition to chemical effect of ultrasound, it has some mechanical effects that result in the destruction of zeolite structure. These effects are detected by XRD patterns and SEM images.

According to the TEM images, there is no good silver nanoparticle distribution on the external surface of zeolite crystals but the process is not complicated and dose not need any reducing agent or surfactants.

Finally, the effect of silver content, type of reaction solution, time of irradiation, and ultrasonic power on the reduction process are studied. The results are summarized as follows:

(1) Lower silver content in the zeolite structure results in the formation of smaller silver nanoparticles on the external surface of the zeolite crystals. Also, the zeolite structure is more destroyed if the samples have more silver content.
(2) The aqueous solution without any additives is a better reaction solution to make higher amount of silver ions reduced and to produce larger particles on the external surface of zeolite structure.
(3) The irradiation time is not an effective parameter to make larger size silver particles on the external surface of zeolite crystals. It may increase slightly the amount of reduction and may result in the more destruction of zeolite structure.
(4) The power of ultrasonic irradiation has a significant effect on the amount of silver ion reduction. By increasing the ultrasonic power, the amount of silver ion reduction increases but there is only a little decrease in the size of silver crystals.

References

1. Chen W, Zhang J, Cai W (2003) Scripta Mater 48:1061
2. Dai WL, Cao Y, Ren LP, Yang XL, Xu JH, Li HX, He HY, Fan KN (2004) J Catal 228:80
3. Cowan MM, Abshire KZ, Houk SL, Evans SM (2003) J Ind Microbiol Biotechnol 30:102
4. Evanoff DD Jr, Chumanov G (2005) Chem Phys Chem 6:1221
5. Kotlyar A, Perkas N, Amirian G, Meyer M, Zimmermann W, Gedanken A (2007) J Appl Sci 104:2868
6. Perelshtein I, Applerot G, Perkas N, Guibert G, Mikhailov S, Gedanken A (2008) Nanotechnology 19:245705
7. Perkas N, Shuster M, Amirian G, Koltypin Y, Gedanken A (2008) J Polym Sci A 46:1719
8. Guczi L (2005) Catal Today 101:53
9. Kumar N, Konova PM, Naydenov A, Heikilla T, Salmi T, Murzin DY (2004) Catal Lett 98(1):57
10. Ju WS, Matsuka M, Iino K, Yamashita H, Anpo M (2004) J Phys Chem B 108:2128
11. Jacobs PA, Uytterhoeven JB (1979) J Chem Soc Faraday Trans 75:56
12. Jacobs PA, Uytterhoeven JB (1977) J Chem Soc Faraday Trans 73:1755
13. Baba T (2005) Catal Surv Asia 9(3):147
14. Sebastian J, Jasra RV (2005) Ind Eng Chem Res 44:8014
15. Tsutsumi K, Takahashi H (1972) Bull Chem Soc Jpn 45:2332
16. Calzaferri G, Suter W, Waldeck B (1990) J Chem Soc Chem Commun 485
17. Liu X, Lampert JK, Arendarskiia DA, Farrauto RJ (2001) Appl Catal B 35(2):125
18. Calmon C, Grundner WT (1968) US Patent 3382039
19. Satokawa S, Kobayashi Y, Fujiki H (2005) Appl Catal B 56 (1–2):51
20. Yang RT, Maldonado AJH, Yang FH (2003) Science 301:79
21. Rosenbach N Jr, Mota CJA (2005) J Braz Chem Soc 16(4):691
22. Wagner GW, Bartram PW (1999) Langmuir 15:8113
23. Shin LK, Kamarudin KSN, Yuan CY, Hamdan H, Mat H (2004) Proceeding of the 18th symposium of malaysian chemical engineering. Malaysia 1:86
24. Chen JH, Lin JN, Kang YM, Yu WY, Kuo CN, Wan BZ (2005) Appl Catal A 291:162
25. Tanabe S, Matsumoto H, Mizushima T, Okitsu K, Maeda Y (1996) Chem Lett 327
26. Okitsu K, Yue A, Tanabe S, Matsumoto H (2002) Bull Chem Soc Jpn 75:449
27. Henglein A (1998) Chem Mater 10:444
28. Zhu J, Liu S, Palchik O, Koltypin Y, Gedanken A (2000) Langmuir 16:6396
29. Zhang Y, Chen F, Zhuang J, Tang Y, Wang D, Wang Y, Dong A, Ren N (2002) J Chem Soc Chem Commun 23:2814
30. Gedanken A (2004) Ultrason Sonochem 11:47
31. Askari S, Halladj R, Nasernejad B (2009) Mater Sci Pol 27(2):397
32. Dion JL (2009) Ultrason Sonochem 16:212
33. Asakura Y, Yasuda K, Kato D, Kojima Y, Koda S (2008) Chem Eng J 139:339
34. Abramov OV, Gedanken A, Koltypin Y, Perkas N, Perelshtein I, Joyce E, Mason TJ (2009) Surf Coat Technol 204:718
35. Okitsu K, Mizokoshi Y, Bandow H, Maeda Y, Yamamoto T, Nagata Y (1996) Ultrason Sonochem 3(3):S249
36. Wang XK, Shao L, Guo WL, Wang JG, Zhu YP, Wang C (2009) Ultrason Sonochem 16:747
37. Fujimoto T, Terauchi SY, Umehara H, Kojima I, Henderson W (2001) Chem Mater 13:1057
38. Nanzai B, Okitsu K, Takenaka N, Bandow H, Tajima N, Maeda Y (2009) Ultrason Sonochem 16:163
39. Okitso K, Ashokumar M, Grieser F (2005) J Phys Chem B 109(4):20673
40. Toshihida B, Noboru A, Mamoru N, Yoshio O (1993) J Chem Soc Faraday Trans 89(3):595